RSC Advances

PAPER

View Article Online
View Journal | View Issue

Cite this: *RSC Adv.*, 2016, **6**, 88057

Improving antifouling ability by site-specific silver decoration on polyethylene ionomer membranes for water remediation: assessed using 3D micro computed tomography, water flux and antibacterial studies

Prasanna Kumar S. Mural,[a] Shubham Jain,[b] Giridhar Madras[c] and Suryasarathi Bose*[b]

Blending immiscible polymer blends often results in coarse microstructures due to interfacial driven coarsening. However, by introducing specific interactions between the constituents, the evolving microstructure can be tailor-made. Herein, water insoluble poly(ethylene-*co*-methacrylic acid) zinc salt (Surlyn) was blended with water soluble polyethylene oxide (PEO) in 50/50 (wt/wt) ratio to construct co-continuous structures that were not possible by blending PE and PEO at the same fraction. By selectively etching the water soluble phase (PEO), porous membranes can be designed with well-defined microstructure as assessed using X-ray micro-computed tomography and the pure water flux across the membranes was studied systematically. In order to impart an antibacterial surface, silver was directly reduced on the membrane surface utilizing the un-neutralized carboxylic acid moieties present in Surlyn as the reducing sites. This led to uniform decoration of silver on the surface which enhanced the antibacterial and antifouling properties. The presence of silver on the membrane was confirmed by X-ray photoelectron spectroscopy (XPS). The distribution of silver and the morphology of the porous Surlyn membrane was evaluated by field emission scanning electron microscopy (FESEM) coupled with EDAX analysis. The antibacterial activity was assessed using a standard plate count method wherein the bacterial cells were in direct contact with the silver decorated membranes. The content of silver present on the surface and the sustained release from the membrane surface was monitored using inductively coupled plasma optical emission spectrometry. The present study opens new avenues in designing efficient and scalable antibacterial membranes.

Received 15th July 2016
Accepted 8th September 2016

DOI: 10.1039/c6ra18043d

www.rsc.org/advances

Introduction

The steep rise in the consumption and contamination of natural water sources, has led to an increasing demand for safe drinking water.[1] Water can be purified by various methods such as disinfection, distillation, and media filtration and separation technology. Membrane separation is favored because there is no requirement for chemical additives, it is less energy intensive and more economical.[2] Pressure driven separation is the most commonly employed method among the various membrane separation technologies.[3,4]

Membrane separation utilizes semipermeable membranes that separate the contaminants. The surface is in direct contact with the incoming feed stream containing particulates and microorganisms. The microorganisms in the feed attach to the membrane surface and cause biofilm formation that tends to foul the membrane over a period of time.[5] Biofilm results in clogging of active pores resulting in increased membrane resistance. Thus, separation technology involves the preparation of membranes and methodology for avoiding biofouling.

Owing to their performance[6] polymeric membranes are preferred over other types of membranes. Polymeric membranes are prepared *via* track etching, stretching melt-cast polymer films, or thermally induced phase separation (TIPS).[7] Commercial membranes are derived from polysulfone, cellulose, polytetrafluoroethylene and polyvinylidene fluoride *etc.*[8] Poly(ethylene-*co*-methacrylic acid) zinc salt (Surlyn) exhibits good transparency with puncture and oil resistance properties.[9] Further, Surlyn contains metal neutralized carboxylate groups or carboxylic groups that can be utilized for further chemical modifications.[10,11] Surlyn chemically coupled with benomyl, benzoic acid and sorbic acid have exhibited enhanced antibacterial activity.[9,12] However, their antibacterial activity was

[a]*Center for Nano Science and Engineering, Indian Institute of Science, Bangalore-560012, Karnataka, India*

[b]*Department of Materials Engineering, Indian Institute of Science, Bangalore-560012, Karnataka, India. E-mail: sbose@materials.iisc.ernet.in*

[c]*Department of Chemical Engineering, Indian Institute of Science, Bangalore-560012, Karnataka, India*

dependent on diffusion of these molecules from the matrix to media. It would be interesting to study the effect of bactericidal activity if they are coated on the surface because of higher release and direct contact. There has been extensive research on the antibacterial surfaces containing silver[13,14] due to their thermal stability and long term antibacterial activity.[15]

The present study focuses on the utilization of Surlyn/PEO blend for preparation of membrane. Further, the free carboxylic acid groups are utilized as a site for reducing silver nitrate to silver on the surface of Surlyn. Extensive work has been done using silver coating, but this study utilizes the specific unneutralized carboxylic acid moieties on the Surlyn surface to bind silver. The silver was determined by XPS and EDAX mapping. The membrane performance and antibacterial activity was assessed systematically. The silver coated membrane opens up new avenues for designing efficient antibacterial membranes using immiscible blends as a model system.

Experimental

Materials

Poly(ethylene-*co*-methacrylic acid) zinc salt (Surlyn) of melting point (T_m) of 89 °C, density of 0.94 g ml^{-1} at 25 °C and melt flow index of 5.5 g/10 min (@190 °C and 2.16 kg), low density polyethylene of melt flow index of 25 g/10 min (@190 °C and 2.16 kg), polyethylene oxide (PEO) (M_v of 400 000 g mol^{-1}) and silver nitrate of 99% purity was procured from Sigma Aldrich. Reducing agent *i.e.* sodium borohydride and all other reagents and solvents of analytical grade were procured and used without any purification.

Membrane preparation

Blends of Surlyn (50 wt%) and PEO (50 wt%) were prepared by melt-mixing using a Polylab, Thermo Haake Minilab II mixer at 150 °C, 60 rpm for 20 min, followed by compression molding to obtain desired shape of membrane coupons. Thus obtained coupons were dipped in cold DI water for 24 h to etch out the PEO phase. The etching of PEO phase generates porous Surlyn membranes.

Surface coating of membranes

To obtain the antibacterial and antifouling properties, Surlyn membranes were coated with silver by chemical reduction of silver nitrate as shown in Scheme 1. The reduction of silver nitrate was carried out by using sodium borohydride as a reducing agent. Prior to coating, the surface was cleaned by sonicating the membrane in acetone to remove surface impurities. After removal of surface impurities, the membrane was transferred to a silver nitrate bath containing different concentrations (of 0.01, 0.10, 0.25, 0.50, 0.75, 1.00, 5.00 and 10.00 wt/vol silver nitrate). The bath containing the membrane was stirred in cold water for 1 h. After 1 h, the appropriate solution containing $NaBH_4$ was added slowly with stirring to prevent agglomeration of silver on the surface. After silver coating, the samples were washed thrice to remove any unattached silver particles on the surface.

Characterization of silver coating on Surlyn membranes

The silver coating on the surface was analyzed by X-ray photoelectron spectroscopy (XPS) by AXIS ULTRA (Kratos Analytical instrument) using monochromatic (Al) source. The silver coating was further confirmed by scanning electron microscopy (SEM) and Energy Dispersive Analysis of X-rays (EDAX) mapping. The membrane morphology and distribution of silver was carried out using field emission scanning electron microscopy (FE-SEM) with EDAX mapping supplied by Carl Zeiss. The 3D tomogram of membranes was obtained by X-ray micro-computed tomography using Xradia Versa XRM 500. The 3D tomograms were generated by combining 1600 projections obtained at X-ray voltage of 80 kV with 25 mm distance between the sample and detector.

Membrane performance

The membrane performance was analyzed by measuring the permeate flow rate (Q) of pure water using the dead end filtration setup. In order to maintain steady flow, initially membranes were compacted at 20 psi for 1 h, and then the pressure was reduced to 10 psi for measurement of permeate flow rate. Flux across the membrane (permeate flux (J)) is calculated by $J = Q/A$, where A is the active membrane area (m^2). The average flux from three samples was checked for consistency.

Antibacterial activity of designed membrane

The antibacterial activity was evaluated by using *Escherichia coli* (*E. coli*) (ATCC 25922) as a model bacterium. The stock culture was further sub cultured for 37 °C in Luria Bertani broth (LB) to obtain fresh culture which was then centrifuged to remove any nutrients from media. The pellet obtained from centrifuging was further re-suspended in phosphate buffered saline (PBS) to obtain the desired cell concentration ($\sim 10^7$ cells per ml). The membranes of desired dimension were suspended in culture containing PBS and were incubated at 37 °C for 1/2 h. The antibacterial efficacy was measured by plating the cells on the nutrient agar. Further, to analyze the morphological feature associated with the attachment of *E. coli*, environmental SEM (E-SEM) was carried out. The *E. coli* was fixed on the membrane surface by 3.7% formaldehyde followed by rinsing with distilled water (DI) and vacuum drying.

Silver release

Silver release over period of time and amount of silver present on the surface of the membrane was determined by using inductively coupled plasma optical emission spectrometry (ICP-OES) supplied by Thermo Scientific iCAP 6000. To obtain the amount of silver present on the surface the silver coated Surlyn membrane was dipped in concentrated HNO_3 and stirred for 1 h. Then the obtained solution was suitably diluted for silver detection using ICP. The silver release was studied by dipping

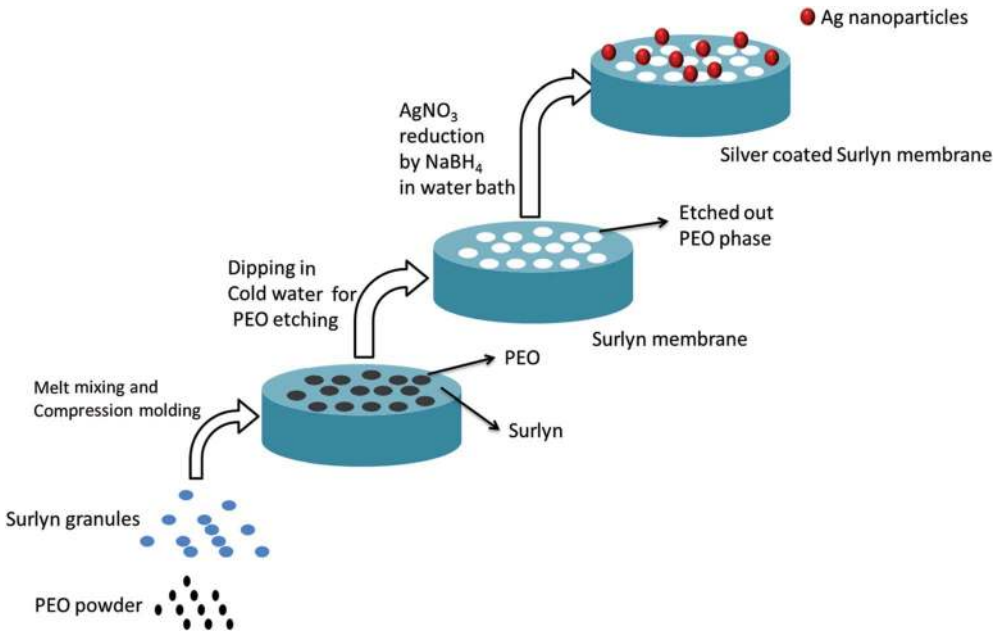

Scheme 1 A cartoon illustrating the membrane preparation, selective etching and silver coating on the token membranes.

the membrane of specific dimension in water for 30 min. The solution was filtered and then the concentration of silver was determined by ICP.

Results and discussion

Tailor-made morphology in Surlyn/PEO blends

The morphology of 50/50 (wt/wt) PE/PEO and Surlyn/PEO (50/50 wt/wt) blends after etching out the PEO phase is shown in Fig. 1 to obtain a clear understanding of the fact as to how the specific interactions between the constituent polymer governs the overall morphology in immiscible systems. It is evident from the micrograph that blends of Surlyn/PEO exhibited typical co-continuous structures, whereas the PE/PEO blend exhibited a typical sea island type of morphology with irregular and discontinuous PEO phase distribution. The blend morphology of PE/PEO is a typical characteristic of immiscible systems where interfacial driven coarsening is quite strong given the large differences in their surface free energy values (PE = 35.3 mN m^{-1} and PEO = 42.9 mN m^{-1} at 20 °C (ref. 16)). By introducing specific interactions between the constituents, finer microstructures can be expected during mixing although to a limited extent in case of only physical/secondary interactions. In case of *in situ* reactive blending, these effects can be well realized in the final blend microstructure. Nevertheless, the weak interaction between Surlyn and PEO has resulted in finer structures as compared to blends of PE/PEO. By selective etching, the contrast can be improved, as observed from these micrographs. The morphology obtained in Surlyn/PEO blends would further attract these structures for exploring them as membrane material as interconnected morphology[5] offers high transport properties and also provides anisotropic pores. The

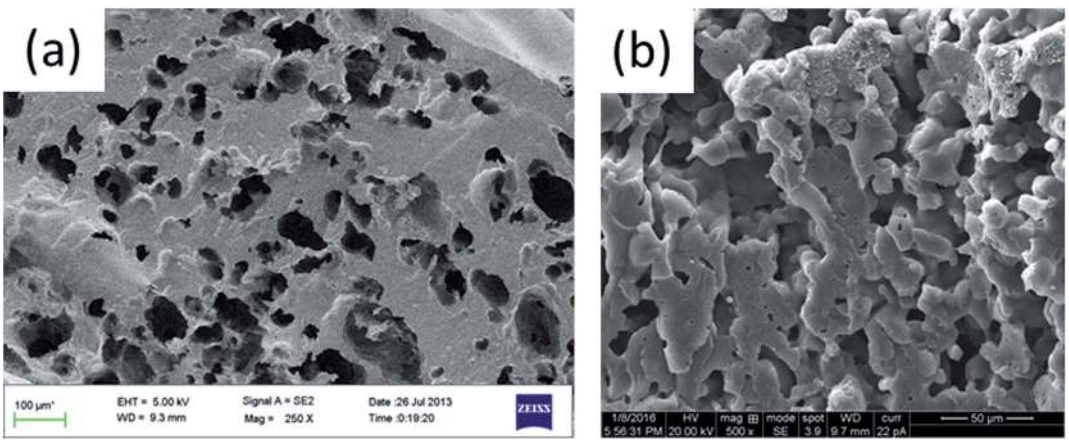

Fig. 1 Morphology of 50/50 (wt/wt) PE/PEO blend (a) and 50/50 (wt/wt) Surlyn/PEO (b).

latter is beneficial for trapping colloids, bacteria and other contaminants present in water.

Silver coating on porous Surlyn membranes

Silver was coated on Surlyn by chemical reduction of silver nitrate using sodium borohydride ($NaBH_4$) as a reducing agent:

$$AgNO_3 + NaBH_4 \rightarrow Ag + 1/2H_2 + 1/2B_2H_6 + NaNO_3$$

The presence of silver on the Surlyn membrane was confirmed by using XPS as shown in Fig. 2. Fig. 2a shows a wide scan of Surlyn membrane with and without silver coating. It is evident that the sample coated with silver exhibited a doublet peak around the binding energy of 368 Ag (3d). The individual scan of silver (Fig. 2b) around 360–380 eV confirmed the doublet peaks at 368.3 and 374.3 eV, corresponding to Ag ($3d_{5/2}$) and Ag ($3d_{3/2}$) respectively. Ag^0 ($3d_{5/2}$) exhibits a peak at 368.3 eV, thus confirming the silver in metallic state.[17] Further, splitting in 3d exhibited a difference of 6.0 eV thus reconfirming the presence of silver in metallic form.[18–20]

Further, grazing angle X-ray diffraction was employed to reconfirm the presence of silver on the token membranes. From Fig. 3, it is evident that Surlyn with silver coating exhibited diffraction peaks at 2θ of 38.0, 44.3, 64.4, 77.3 and 81.5 corresponding to the index of [111], [200], [220], [311] and [222] planes of pure silver (JCPDS card no. 00-04-0783). This reconfirms the effective silver coating on the Surlyn surface.[21]

Fig. 4a and b exhibit the SEM micrographs of token Surlyn membranes before and after silver coating. Fig. 4b shows silver particles distributed across the surface of the token membranes. Further, Fig. 4c shows the micrograph of silver coated Surlyn membrane with corresponding EDAX spectra and silver mapping. From Fig. 4c, it is evident that silver is distributed well across the membrane surface and more importantly, around the pores and thus suggesting uniform distribution of silver on the surface.

Assessing the porous morphology using 3D micro-computed tomography

The Scheme 2 shows the X-ray tomography projections obtained for generation of 3D profile of the designed membrane. Fig. 5a shows the reconstructed 3D tomography of 50/50 (wt/wt) PE/PEO blend after etching out the PEO phase, it is evident that the blend exhibits the sea island type of morphology with irregular and discontinuous PEO phase distribution which is in line with SEM micrograph discussed earlier. On the contrary, the 50/50 (wt/wt) Surlyn/PEO blend (Fig. 5b) exhibit co-continuous type of morphology wherein anisotropic pores with interconnected structures is well evident from the 3D images. The interconnected structures offer high transport properties along with anisotropic pores which assist in trapping colloids, bacteria and other contaminants present in water.

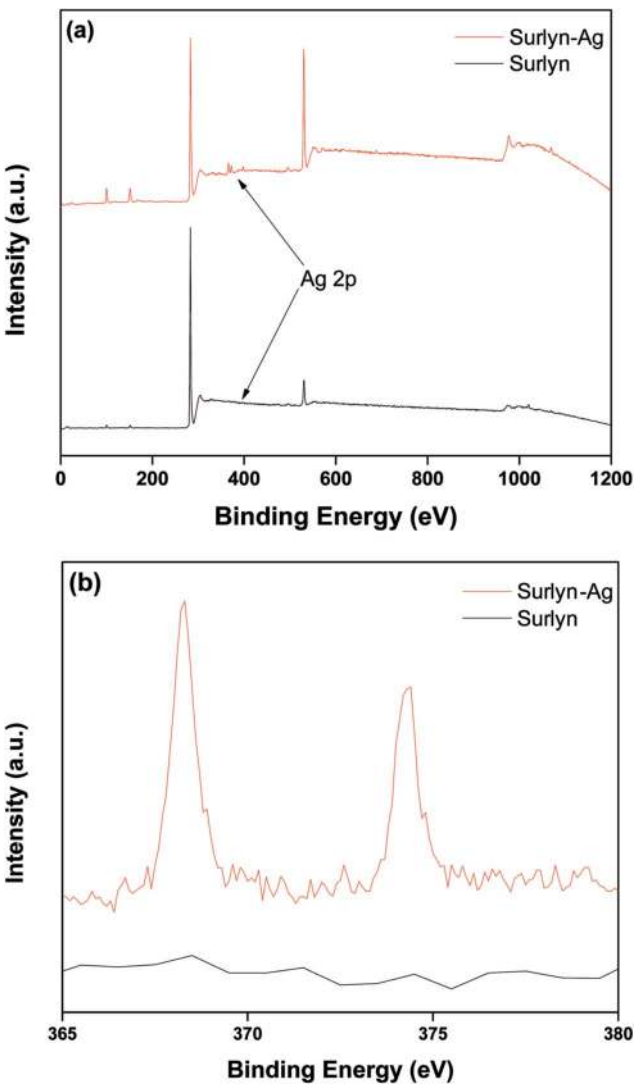

Fig. 2 XPS wide scan (a) and Ag-3d spectra (b) of Surlyn membrane with and without silver coating.

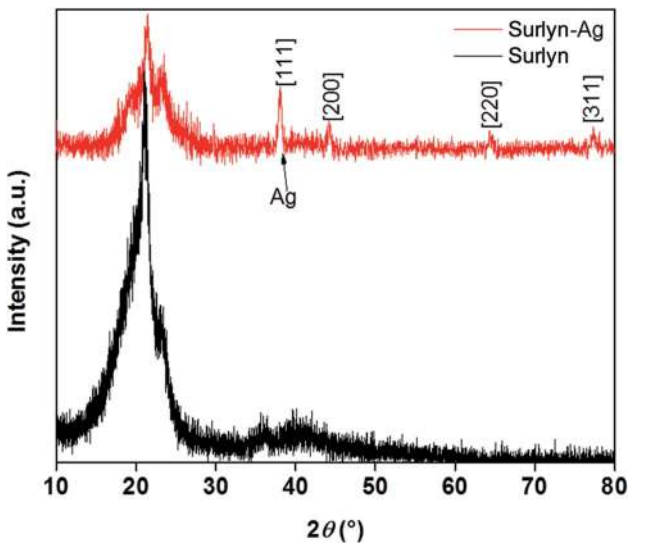

Fig. 3 The grazing angle XRD pattern of Surlyn with and without silver coating.

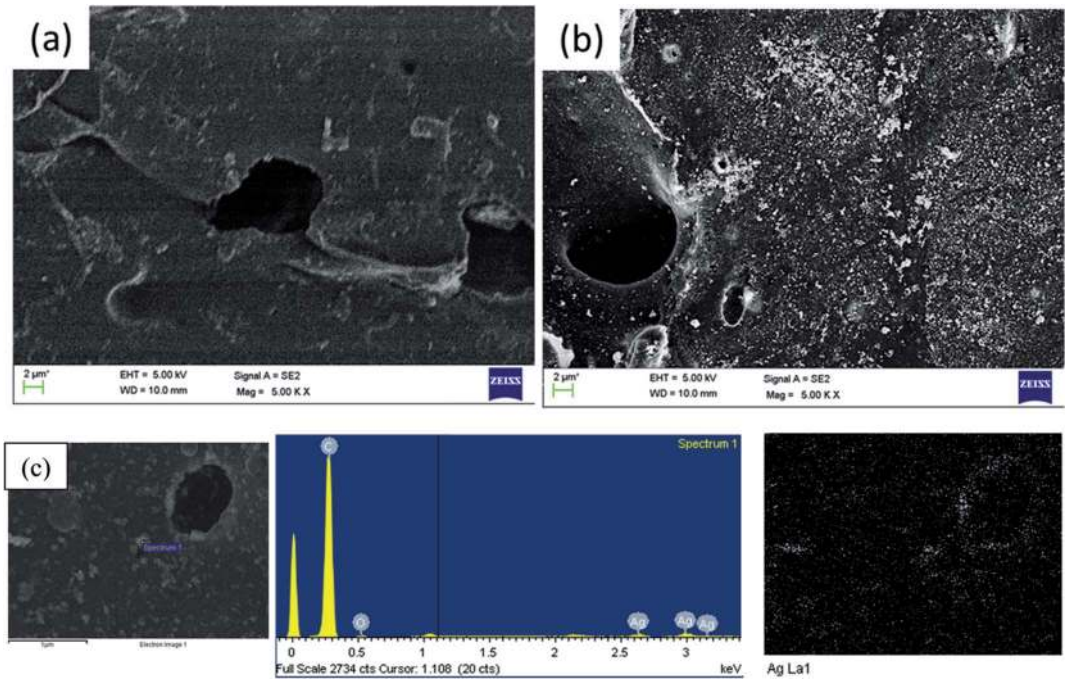

Fig. 4 Morphology of Surlyn membrane without (a) and with (b) silver coating and magnified morphology coupled with EDAX and mapping of silver coated Surlyn membrane (c).

Further, the silver coating (Fig. 5c) on the surface provides the advantages of bactericidal effect to kill bacteria on the surface of the membrane. However, it is can be noted that higher loading of silver, for instance, when 10 wt/vol silver nitrate was reduced onto the surface, they tend to form clusters around the edges of the pore. These clusters can obstruct the flow of water, which increases the resistance of membrane. This observation is consistent with the decreased flux across the membrane, which is discussed in the subsequent section.

Membrane performance

The membrane performance was assessed by in-house designed dead-end membrane setup with a inlet pressure of 10 psi. Fig. 6 shows the flux across the membrane wherein the neat token membranes exhibited a flux of 12 240 $\pm$ 360 L m^{-2} h^{-1}. Further, with 0.01 wt/vol silver coating the flux reduced to 9452 $\pm$ 1200 L m^{-2} h^{-1} which is due to surface coating of silver present on the surface which possibly has increased the resistance. Further increasing the silver coating *i.e.* 0.1, 0.25, 0.50, 0.75, 1.00, 5.00 and 10.00 wt/vol reduces the flux to 8243 $\pm$ 550 L m^{-2} h^{-1}, 8052 $\pm$ 450 L m^{-2} h^{-1}, 7550 $\pm$ 430 L m^{-2} h^{-1}, 7380 $\pm$ 540 L m^{-2} h^{-1}, 6588 $\pm$ 1440 L m^{-2} h^{-1}, 4680 $\pm$ 432 L m^{-2} h^{-1} and 1044 $\pm$ 360 L m^{-2} h^{-1} respectively. Thus, from Fig. 6, one can conclude that an increase in silver concentration results in the reduction of flux across the membrane. This decrease in flux is attributed to the increase in resistance. As observed earlier, clusters around the pores was observed at

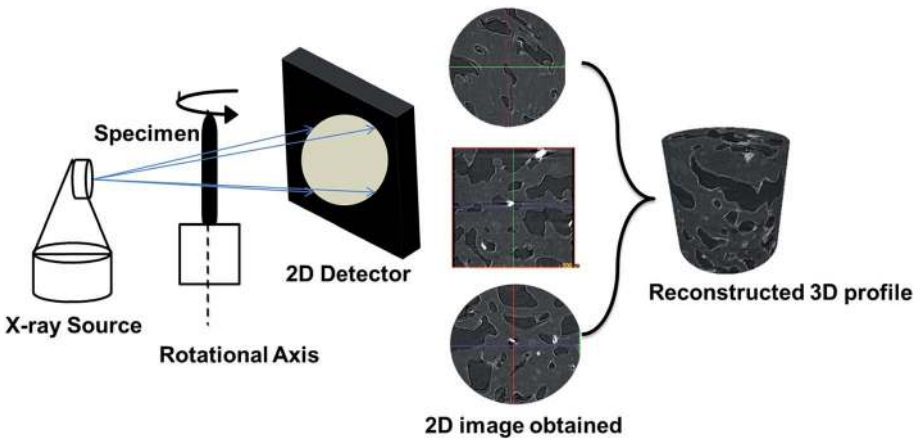

Scheme 2 Schematic representation of X-ray tomography projections obtained for generation of 3D profile.

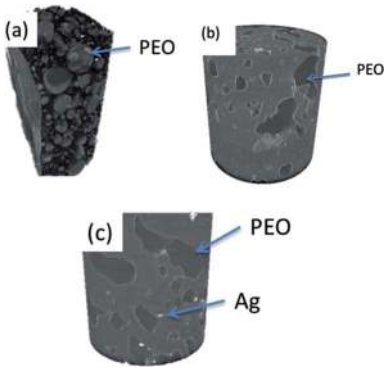

Fig. 5 Representative 3D re-constructed images of 50/50 wt/wt blends of PE/PEO (a), Surlyn/PEO without silver coating (b) and with silver coating (c).

higher silver content. This clustering around the edges results in partial blockage of water flow thus increasing the resistance offered by the membrane. The increase in resistance results in the decrease in flux. The clustering of silver particles around the edges of the pore can be observed from Fig. 4c illustrating the EDAX mapping. Thus, based on the flux reduction with increase in silver coating, one can conclude that there is tradeoff between the amount of silver coating and flux *i.e.* silver concentration plays a key role in obtaining better flux. However, with increasing silver content, the bactericidal activity can be increased at the cost of decreased flux. Further, the silver release during filtration attracts standard regulatory bodies as the maximum permissible limit of silver content in water is 0.1 ppm as per World Health Organization (WHO).[22] The silver release during separation process was studied systematically (to be discussed in the subsequent section) to optimize the silver content, bactericidal effects and flux that meets the WHO recommendation *i.e.* 7 log reduction in bacteria.

Antibacterial activity

The antibacterial activity of the membranes was evaluated using *E. coli* (Gram negative) as a model bacterium. Fig. 7 shows the colony forming units (CFU per ml) on various token samples after inoculation. It is evident from Fig. 7 that a 7 log reduction in colony forming unit was observed beyond certain silver concentration of the coated membrane samples after 30 min of inoculation. Further, the initial cell concentration of $6.2 \pm 0.5 \times 10^7$ CFU per ml after incubation for 1/2 h inoculation with membrane showed a $4.5 \pm 1.6 \times 10^7$ CFU per ml (as shown in Fig. 8). Further, culture without any membrane (positive control) *i.e.* culture without any samples exhibited $3.44 \pm 0.35 \times 10^7$ CFU per ml suggesting no significant reduction in colonies of the neat membrane. Further, with the increase of silver coating content the antibacterial activity increased, which resulted in the reduction of colonies. For 0.01 wt/vol silver coating exhibited bactericidal efficacy of 38%, similarly for 0.10, 0.25 and 0.75 wt/vol silver coating a bactericidal efficacy of 62%, 88% and 99.7% respectively was observed. For 1.00, 5.00, 10.00 wt/vol silver coating, a bactericidal efficacy of 100% (which is 7 log reductions in bacterial activity) was observed. Hence a 100% reduction in all silver coated membranes was observed in just 30 min.

Further to assess the possible mechanism of the antibacterial activity, SEM and silver release studies were carried out by ICP-OES. Direct contact of silver attached on the surface of membrane with bacteria can be probed by fixing the cells on the membrane surface. Fig. 9 shows the micrograph of bacteria adhered to the membrane surface. The membranes without silver coating showed the bacteria with intact cell wall attached to the surface (Fig. 9a). Further, Fig. 9b shows the bacteria with cell wall distorted/disturbed in the presence of silver. This is manifested due to leakage of intercellular fluid in contact with silver resulting in cell death. Further, from ICP-OES (discussed in subsequent section), it is evident that there is a sustained

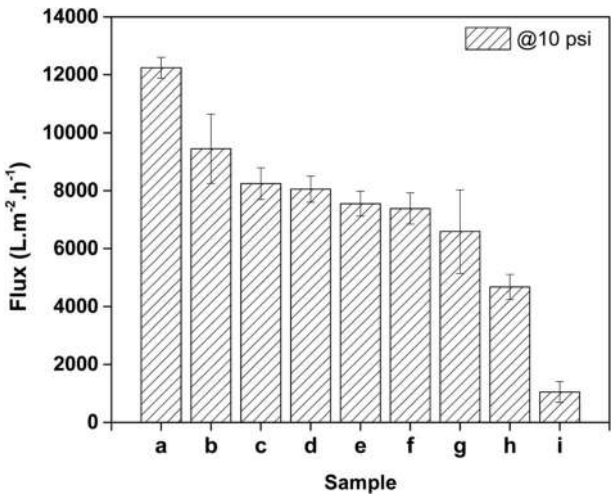

Fig. 6 Membrane performance (flux across the membrane) of Surlyn membrane (a) and (0.01 (b), 0.10 (c), 0.25 (d), 0.50 (e), 0.75 (f), 1.0 (g), 5.0 (h) and 10.0 (i) wt/vol) silver coated Surlyn membrane.

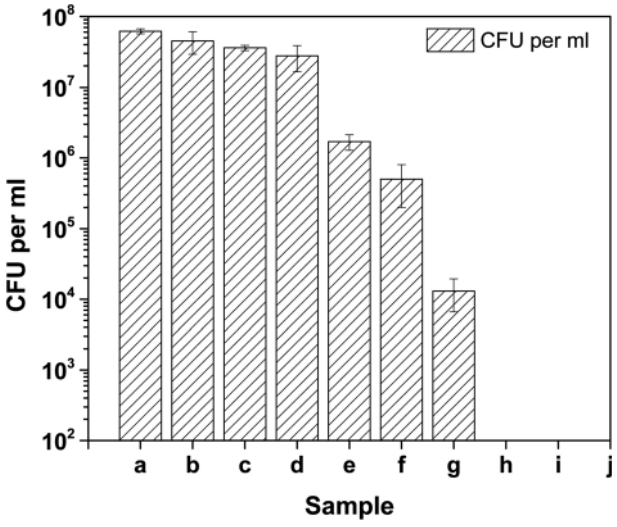

Fig. 7 Colony forming unit (CFU) per ml of Surlyn membranes without (blank (a), and neat (b)) and with (0.01 (c), 0.1 (d), 0.25 (e), 0.50 (f), 0.75 (g), 1 (h), 5 (i) and 10 (j) wt/vol) silver coating.

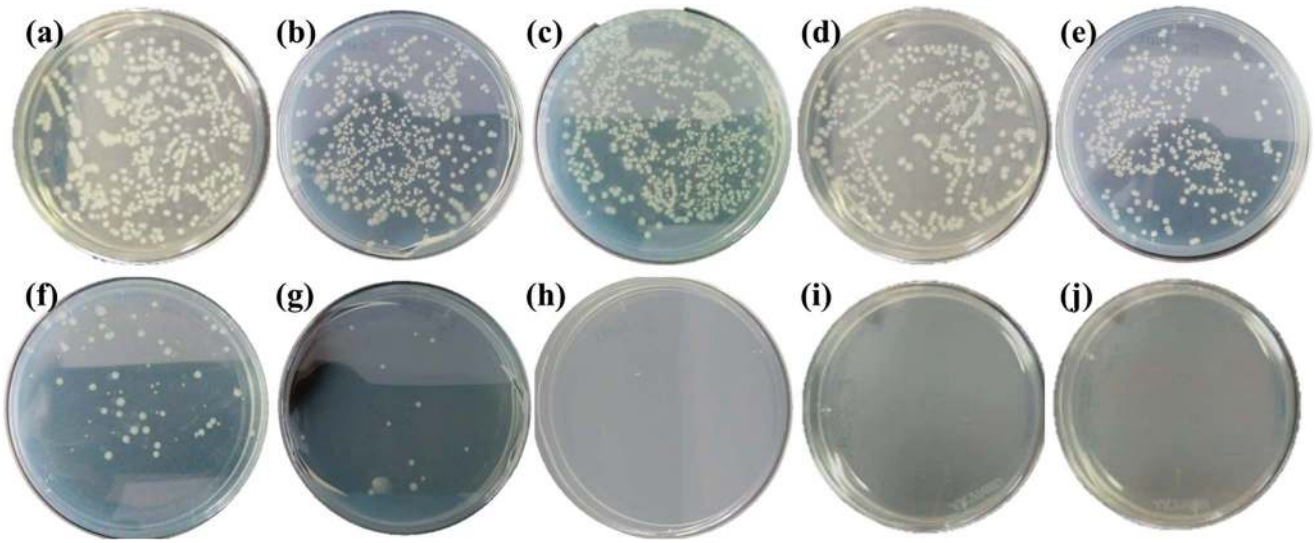

Fig. 8 Total agar plate counts of bacterial colonies of token Surlyn membranes; negative control (a), control blends (b) and with 0.01 (c), 0.1 (d), 0.25 (e), 0.50 (f), 0.75 (g), 1.0 (h), 5.0 (i) and 10.0 (j) wt/vol silver coating.

release of silver ions, which resulted in antibacterial activity. However, the higher release of silver ions is not recommended.[23] Thus, it is important for a sustained release of silver. Based on our results, one can optimize that 1% wt/vol silver coating provides the required antibacterial activity and also meets the required standards of silver release. Li *et al.* reported that the release of Ag^{+} ions causes the disruption of cell membrane, electron transportation and DNA damage.[24] Thus, upon contact with silver present on the membrane surface, the bacteria cell membrane distorts which create pits[25] in cell wall resulting in release of intercellular fluids; finally leading to lysis. The silver on the sample attaches to the cell membrane due to electrostatic interaction between the negative charge cell membrane (due to peptidoglycan layer) and positively charge silver. Further, the silver release causes the depletion of silver from surface leading to pit formation from where the intercellular fluid releases causing the lysis of cell. The release of silver ions to media causes silver to bind to the sulfhydryl groups, thus leading to reduction of disulfide bonds, which results in denaturation of proteins in DNA.[26,27] Further, the silver ion forms a complex with groups like oxygen, nitrogen or sulfur which are electron donor present in nucleic acids and amino acids (as phosphates or thiols). Thus, silver binding on to these groups result in the disruption of electron transportation[28–30] which further leads to lysis of cell.

Further, to show the release of silver from the membrane surface, the ICP-OES was carried out. Firstly, the amount of silver present on the surface was evaluated by dissolving the silver present on the membrane surface using HNO_3. Table 1 lists the total quantity of silver content on the member surface after complete removal. It is evident from Table 1 that silver content scaled with the content of initial silver loading. This

Table 1 Quantity of silver present on the membrane after complete removal of silver

Sample	Quantity of silver ($\mu g\ mm^{-2}$)
Membrane with 0.01 wt/vol silver coating	3.5 ± 1.1
Membrane with 0.10 wt/vol silver coating	7.2 ± 2.4
Membrane with 0.25 wt/vol silver coating	10.5 ± 1.2
Membrane with 0.50 wt/vol silver coating	34.5 ± 2.7
Membrane with 0.75 wt/vol silver coating	46.8 ± 1.6
Membrane with 1 wt/vol silver coating	135.1 ± 1.8
Membrane with 5 wt/vol silver coating	219.5 ± 2.3
Membrane with 10 wt/vol silver coating	270.4 ± 5.3

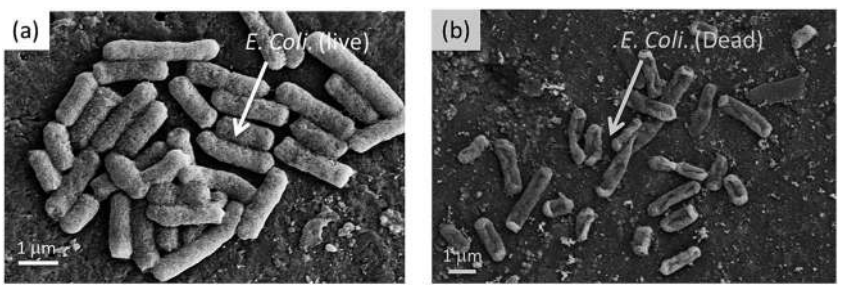

Fig. 9 SEM morphology of Surlyn membrane (a) and with 10 wt/vol Ag coating (b).

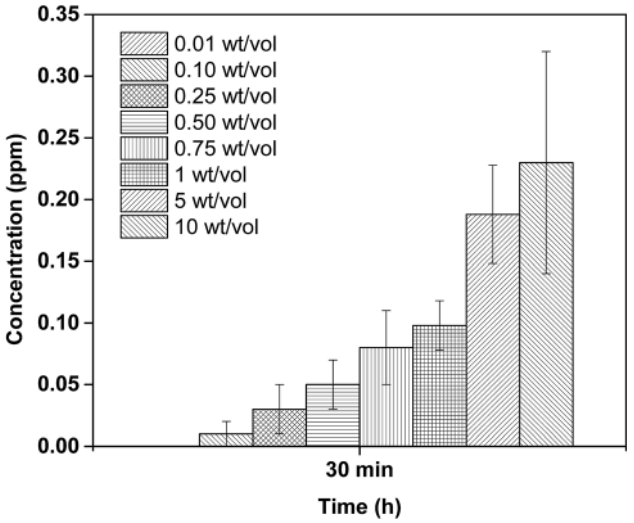

Fig. 10 Silver release from the silver coated Surlyn membranes.

explains the increased resistance to water flow with increased amount of silver present on the token membrane surface. This is manifested from the reduced flux as discussed earlier. The antibacterial activity is strongly dependent on the release of silver and thus the silver release was assessed as function of concentration. Further, Indian standard specifies that for drinking water maximum permissible limit of silver is 0.1 mg l^{-1}.[23] From Fig. 10, it evident that the 1 wt/vol silver coated membrane exhibits the silver release under the permissible limit with 100% bacterial efficacy.

Conclusions

The present study demonstrates the successful development of Surlyn (partially neutralized zinc salt of polyethylene) based porous membranes by selectively etching the water soluble PEO phase from the Surlyn/PEO (50/50 wt/wt) blends. The un-neutralized –COOH groups further helped in reducing silver nanoparticles on the porous membranes. The specific interaction between the constituents resulted in co-continuous structures. The interconnected structures further offered high transport properties through the anisotropic pores which assisted in trapping colloids, bacteria and other contaminants present in water. The silver coating on the token membranes resulted in significant bactericidal activity though the silver concentration on the membrane surface played an important role. There is a trade-off between the increase in resistance (due to silver coating) and the bactericidal effect. The release of silver ions from the token membranes was systematically studied and for an optimum membrane, the release met the standards recommend for safe drinking water. Hence, the designed membranes open new avenues in designing scalable antibacterial membranes.

Acknowledgements

The authors would like to acknowledge the financial support from Department of Science and Technology, characterization facilities of MNCF, CeNSE and Materials Engineering Department Dr Ramananda Chakrabarti of Center for Earth Sciences for assisting in ICP analysis and Prof. Jayant Modak of Chemical Engineering Department, IISc for bacterial studies.

References

1 M. A. Shannon, P. W. Bohn, M. Elimelech, J. G. Georgiadis, B. J. Marinas and A. M. Mayes, Science and technology for water purification in the coming decades, *Nature*, 2008, **452**, 301–310.
2 M. M. Pendergast and E. M. V. Hoek, A review of water treatment membrane nanotechnologies, *Energy Environ. Sci.*, 2011, **4**, 1946–1971.
3 R. E. Kesting, The four tiers of structure in integrally skinned phase inversion membranes and their relevance to the various separation regimes, *J. Appl. Polym. Sci.*, 1990, **41**, 2739–2752.
4 M. Ulbricht, Advanced functional polymer membranes, *Polymer*, 2006, **47**, 2217–2262.
5 P. K. S. Mural, S. Jain, S. Kumar, G. Madras and S. Bose, Unimpeded permeation of water through biocidal graphene oxide sheets anchored on to 3D porous polyolefinic membranes, *Nanoscale*, 2016, **8**, 8048–8057.
6 A. Mehta and A. L. Zydney, Permeability and selectivity analysis for ultrafiltration membranes, *J. Membr. Sci.*, 2005, **249**, 245–249.
7 G. M. Geise, H.-S. Lee, D. J. Miller, B. D. Freeman, J. E. McGrath and D. R. Paul, Water purification by membranes: the role of polymer science, *J. Polym. Sci., Part B: Polym. Phys.*, 2010, **48**, 1685–1718.
8 P. K. S. Mural, A. Banerjee, M. S. Rana, A. Shukla, B. Padmanabhan, S. Bhadra, G. Madras and S. Bose, Polyolefin based antibacterial membranes derived from PE/PEO blends compatibilized with amine terminated graphene oxide and maleated PE, *J. Mater. Chem. A*, 2014, **2**, 17635–17648.
9 Y.-M. Weng, M.-J. Chen and W. Chen, Antimicrobial food packaging materials from poly(ethylene-*co*-methacrylic acid), *LWT–Food Sci. Technol.*, 1999, **32**, 191–195.
10 K. Han and H. L. Williams, Ionomers: the sodium salt of poly(ethylene-*co*-methacrylic acid), *J. Appl. Polym. Sci.*, 1989, **38**, 73–86.
11 S. Seethamraju, P. C. Ramamurthy and G. Madras, Ionomer Based Blend as Water Vapor Barrier Material for Organic Device Encapsulation, *ACS Appl. Mater. Interfaces*, 2013, **5**, 4409–4416.
12 G. W. Halek and A. Garg, Fungal inhibition by a fungicide coupled to an ionomeric film, *J. Food Saf.*, 1988, **9**, 215–222.
13 R. Carbon, S. Lugauer, U. Geitner, A. Regenfus, M. Böswald, J. Greil, T. Bechert, S.-I. Simon, H. Hümmer and J.-P. Guggenbichler, Reducing catheter-associated infections with silver-impregnated catheters in long-term therapy of children, *Infection*, 1999, **27**, S69–S73.
14 M. E. Olson, B. G. Harmon and M. H. Kollef, Silver-coated endotracheal tubes associated with reduced bacterial

burden in the lungs of mechanically ventilated dogs, *Chest*, 2002, **121**, 863–870.

15 A. Sadeghnejad, A. Aroujalian, A. Raisi and S. Fazel, Antibacterial nano silver coating on the surface of polyethylene films using corona discharge, *Surf. Coat. Technol.*, 2014, **245**, 1–8.

16 P. K. S. Mural, G. Madras and S. Bose, Positive temperature coefficient and structural relaxations in selectively localized MWNTs in PE/PEO blends, *RSC Adv.*, 2014, **4**, 4943–4954.

17 E.-J. Lee, L. Piao and J.-K. Kim, Synthesis of Silver Nanoparticles from the Decomposition of Silver(I)[bis (alkylthio)methylene]malonate Complexes, *Bull. Korean Chem. Soc.*, 2012, **33**, 60–64.

18 P. K. S. Mural, M. Sharma, A. Shukla, S. Bhadra, B. Padmanabhan, G. Madras and S. Bose, Porous membranes designed from bi-phasic polymeric blends containing silver decorated reduced graphene oxide synthesized *via* a facile one-pot approach, *RSC Adv.*, 2015, **5**, 32441–32451.

19 A. Barrie and N. Christensen, High-resolution X-ray photoemission spectra of silver, *Phys. Rev. B: Solid State*, 1976, **14**, 2442.

20 M. Sharma, N. Padmavathy, S. Remanan, G. Madras and S. Bose, Facile one-pot scalable strategy to engineer biocidal silver nanocluster assembly on thiolated PVDF membranes for water purification, *RSC Adv.*, 2016, **6**, 38972–38983.

21 C. Liu, X. Yang, H. Yuan, Z. Zhou and D. Xiao, Preparation of Silver Nanoparticle and Its Application to the Determination of ct-DNA, *Sensors*, 2007, **7**, 708–718.

22 T. A. Dankovich and D. G. Gray, Bactericidal paper impregnated with silver nanoparticles for point-of-use water treatment, *Environ. Sci. Technol.*, 2011, **45**, 1992–1998.

23 I. Standard, *Drinking water-specification*, 1st Revision, IS, 1991, p. 10500.

24 Q. Li, S. Mahendra, D. Y. Lyon, L. Brunet, M. V. Liga, D. Li and P. J. Alvarez, Antimicrobial nanomaterials for water disinfection and microbial control: potential applications and implications, *Water Res.*, 2008, **42**, 4591–4602.

25 J. S. Kim, E. Kuk, K. N. Yu, J.-H. Kim, S. J. Park, H. J. Lee, S. H. Kim, Y. K. Park, Y. H. Park and C.-Y. Hwang, Antimicrobial effects of silver nanoparticles, *Nanomedicine*, 2007, **3**, 95–101.

26 M. Eterpi, G. McDonnell and V. Thomas, Disinfection efficacy against parvoviruses compared with reference viruses, *J. Hosp. Infect.*, 2009, **73**, 64–70.

27 N. V. Ayala-Núñez, H. H. L. Villegas, L. d. C. I. Turrent and C. R. Padilla, Silver nanoparticles toxicity and bactericidal effect against methicillin-resistant *Staphylococcus aureus*: nanoscale does matter, *NanoBiotechnology*, 2009, **5**, 2–9.

28 M. Starodub and J. Trevors, Silver resistance in *Escherichia coli* R1, *J. Med. Microbiol.*, 1989, **29**, 101–110.

29 C.-N. Lok, C.-M. Ho, R. Chen, Q.-Y. He, W.-Y. Yu, H. Sun, P. K.-H. Tam, J.-F. Chiu and C.-M. Che, Proteomic analysis of the mode of antibacterial action of silver nanoparticles, *J. Proteome Res.*, 2006, **5**, 916–924.

30 I. Sondi and B. Salopek-Sondi, Silver nanoparticles as antimicrobial agent: a case study on *E. coli* as a model for Gram-negative bacteria, *J. Colloid Interface Sci.*, 2004, **275**, 177–182.